



Effect of PLA Crystallization on the Thermal Conductivity and Breakdown Strength of PLA/BN Composites

Lu Bai, Shaodi Zheng, Ruiying Bao, Zhengying Liu, Mingbo Yang and Wei Yang*

Poly lactide (PLA), whose crystallinity could be easily tuned, was selected to examine the effect of polymer crystallization on thermal conductivity (TC) of the polymer composites. Compression-molded PLA/boron nitride (BN) were heat-treated at 120 °C to fabricate highly crystalline samples. It demonstrated crystallization of the PLA significantly affects TC of the PLA/BN composites. With increased BN content, the improvement of the TC of PLA/BN composites via crystallization is more obvious. TCs of the crystalline PLA/BN composites with 5 wt% and 40 wt% BN are increased by 23 % and 47 % in the in-plane direction and are increased by 21 % and 54 % in the through-plane direction compared to those of amorphous PLA/BN, while TC of pure PLA is increased by 17 % via crystallization. When BN content is 40 wt%, the in-plane and through-plane TCs of the crystalline PLA/BN are 4.7 W/mK and 0.8 W/mK, respectively. Both the amorphous and crystallized PLA/BN exhibit high breakdown strengths.

Keywords: Thermal conductivity; PLA/BN composite; Crystallization; Breakdown strength

Received 12 December 2018, **Accepted** 29 December 2018

DOI: 10.30919/esmm5f195

1. Introduction

With the continuous miniaturization and integration of microelectronics and emergence of new applications, thermal dissipation is becoming increasingly critical for the performance, lifetime, and reliability of electronic devices.^{1,2} Thus, the exploitation of effective thermal management materials is urgently needed to help address this challenge. Polymer materials with enhanced thermal conductivity (TC) have become some of the most popular thermal management materials due to their advantages of good processability, low weight, high electrical resistivity, high voltage breakdown strength and most importantly, low cost. However, bulk polymers generally exhibit very low TC in the range of 0.1–0.5 W/mK,^{3,4} necessitating the development of highly thermally conductive polymer-based materials to meet increasing demands,^{5,8} which is highly challenging.

Typically, introducing highly heat-conductive fillers, such as carbon-based materials,^{9,13} ceramic fillers,^{14,15} and metallic fillers,^{16,17} into polymers to increase the TC of polymer composites has been the conventional approach both in scientific research and industrial applications. Among these fillers, hexagonal boron nitride (BN) that has a structure analogous to that of graphite, not only has an extraordinary intrinsic TC, but is also an excellent electrical insulator. Therefore, BN has been widely used as an ideal filler to fabricate highly thermally conductive and electrically insulating polymer composites.^{18–20} Actually, the TC of polymer composites depends on the TCs of both polymers

and fillers. However, most attention has been devoted to studying the influences of fillers and the morphological structure of the composites on TC of the composites, such as filler loading,²¹ filler shape,²² particle size,²³ and interfacial interaction between the fillers and matrix.²⁴ The intrinsic performance of the polymer which plays a crucial role in the overall TC of polymer composites is often neglected in the design of highly thermally conductive polymer composites.

Researchers have shown that the crystallinity^{25–28} and molecular orientation^{29–32} strongly affect the TC of polymers. But the effect of crystallization and molecular orientation of polymer matrix on the TC of polymer-based composite cannot be deduced directly from the results of pure polymers. However, few reports on the effect of polymer crystallization on the TC of polymer composites are available.^{33,34} Zhang *et al.*³⁴ reported that the TC of polyethylene/BN composites was improved by controlling the crystallization of the polyethylene (PE) matrix. The results show that the TC of the composites is increased with increasing crystallinity of the PE matrix, and the stable crystals of PE were more favorable for enhancing the TC of the PE/BN composites.

Poly lactide (PLA) is a promising environmentally friendly polymer material,^{35,37} and the development of the application of environmentally friendly materials becomes more and more important.^{38–41} But low thermal conductivity of PLA restricts its applications in engineering and electronic fields and the influences of some basic features of PLA itself on the thermal conductivity have not been well-understood. By taking advantage of very low crystallization kinetics, a wide range of degrees of crystallinity of PLA can be easily achieved by carrying out isothermal crystallization for different periods of time.⁴² The effect of crystallinity on the TC of PLA has been systematically studied in our previous work.⁴³ The results show that TC of PLA increases with increasing crystallinity, but the increment is not significant. To expand the applications of PLA materials, many studies have been conducted to

College of Polymer Science and Engineering, Sichuan University, State Key Laboratory of Polymer Materials Engineering, Chengdu, 610065, Sichuan, China

*E-mail: weiyang@scu.edu.cn

improve the TC of PLA by means of compounding with thermally conductive fillers,^{44,49} which were generally focused on the fillers and did not pay enough attention to the PLA matrix. Thus, it is necessary to elucidate the effect of crystallization on the TC of PLA-based composites.

In this work, BN with different mass ratio was melt compounded into PLA matrix by twin-screw extrusion. Two series of PLA/BN composites with highly crystalline PLA matrix and amorphous PLA were fabricated via compression molding at 190 °C for 3 min. One of these was then heat-treated at 120 °C for 20 min while the other one was not. Morphology of the composites, crystallinity of the PLA matrix, filler orientation, TC and breakdown strength of the as-prepared composites were comprehensively examined and the effect of PLA crystallization on the TC of PLA/BN composites was discussed.

2. Experimental Section

2.1 Materials and sample preparation

PLA (trade name 4032D, Nature Works LLC) was used as the polymer matrix. The weight average molecular weight (Mw) and the polydispersity index (PDI) of PLA are 2.1×10^5 g/mol and 1.7, respectively. Hexagonal boron nitride (h-BN) with the lateral size of 10–15 μm and purity of 99.0 % was supplied by Eno Material, China. PLA granules and BN fillers were dried in an oven at 60 °C for 12 hrs, then melt compounded in a twin-screw extruder with a rotational speed of 180 rpm at 190 °C. Then, the extruded composites were compressed into sheets with a thickness of approximately 0.5 mm at 190 °C for 3 min under a pressure of 10 MPa. The melted PLA and PLA composites were immediately transferred to crystallize isothermally at 120 °C for 0 min or 20 min under a pressure of 10 MPa and then cooled rapidly to obtain amorphous or crystallized samples that were designated as BNX and BNX-20, where X represents the weight fraction of BN (0, 5, 10, 20, 30 and 40 wt%) in the composites.

2.2 Characterization

2.2.1 Differential scanning calorimetry (DSC)

PLA and PLA/BN composites were examined by DSC (Q20, TA Instruments, USA) from 40 °C to 190 °C with a heating rate of 10 °C/min under a nitrogen gas flow of 50 mL/min. The degree of crystallinity of PLA and the composites is calculated using Eq.(1).

$$X_c = 100\% \times (\Delta H_m - \Delta H_{cc})/\Delta H_{100} \quad (1)$$

where ΔH_{100} represents the melting enthalpy of a 100 % crystalline PLA, and is taken to be 93 J/g⁵⁰.

Specific heat measurements of all the samples were performed by DSC in the modulated mode (Q20, TA Instruments, USA) in the temperature range of 0 - 50 °C at a heating rate of 3 °C/min under a nitrogen gas flow of 50 mL/min.

2.2.2 Scanning electron microscopy (SEM)

Cross-sections of all the samples were prepared by fracturing after the samples were immersed in liquid nitrogen for 30 min. After coating with gold, the fractured surfaces were observed with an SEM (Inspect F, FEI Company, USA) operating at an accelerating voltage of 5 kV.

2.2.3 X-ray diffraction (XRD) measurement

XRD patterns of PLA and PLA/BN compression molded sheets were recorded with a Rigaku Ultima IV diffractometer using a Cu K α radiation source ($\lambda=0.154$ nm, 40 kV, 25 mA) in the scanning range of $2\theta = 10\text{--}90^\circ$ at a scan speed of 10 °/min at room temperature. Measurements were performed for both in-plane and through-plane

directions (Fig. S1) for each sample.

2.2.4 Density measurement

The density of the PLA/BN composites was measured using an MH-120E density meter according to the Archimedes principle.

2.2.5 Thermal diffusivity measurement

Round BNX and BNX-20 disks with the diameters of 12.7 and 25.4 mm, respectively, were cut for through-plane and in-plane thermal diffusivity tests, respectively. Prior to testing, the thickness and diameter of samples were measured, and both surfaces of the samples were evenly sprayed with a thin graphite layer. The samples were then fixed according to the required test pattern and placed in the test chamber at 25 °C (LFA467, Netzsch, Germany).

2.2.6 Infrared thermal imager characterization

An infrared thermal imager (Fluke Ti27) was used to measure the temperature variation of an LED (1 W) with the thermal conductive composites as the heat dissipation substrate when the LED was turned on. Then, software (SmartView 3.6) was used to capture the temperature of LED within 5 min.

2.2.7 Breakdown strength test

The AC dielectric strength was measured using a Beijing Guance DDJ-50K instrument with round disks (ϕ 25.4 mm) cut directly from the composite plates. The specimens were inserted between a pair of spherical brass electrodes with a diameter of 25 mm and then the whole system was immersed in the electrical insulating oil, serving as insulating medium. During testing, the voltage was raised at a rate of 0.2 kV/s. The applied voltages at breakdown were then normalized according to the sample thickness in order to express the breakdown strength in kV/mm.

3. Results and Discussion

Figs. 1(a) and 1(b) show the first heating curves of PLA and PLA/BN composites without and with the isothermal treatment at 120 °C for 20 min, respectively. Significant cold crystallization of the amorphous regions of all of the samples without the isothermal treatment was observed during the heating ramp (Fig. 1a). In contrast, the cold crystallization phenomena completely disappear for the PLA/BN composites with the isothermal treatment. This indicates that the crystallinity of PLA and PLA/BN composite was strongly improved by isothermal treatment at 120 °C for 20 min. The crystallinity values calculated using Eq. (1) are listed in Table 1. It is observed that PLA in PLA/BN composites with different BN contents without the isothermal treatment show very low crystallinity and can be considered as amorphous. After 20 minutes of isothermal crystallization at 120°C, the crystallinity of PLA in PLA/BN composites increased significantly, reaching as high as 50 %. It was also found that the differences between the crystallinity values of PLA were very small despite the different BN content. This means that series of amorphous and crystallized composite materials were prepared successfully, providing good samples for the study of the effect of crystallization on the TC of the composites.

The SEM images of the cross-sections of the PLA/BN composites are shown in Fig. 2 (5 % & 40 % BN) and Fig. S2 (10 %, 20 % & 30 % BN). It is observed that whether the composites were isothermally treated at 120 °C or not, the majority of BN flakes are aligned along the in-plane direction of the sample under the pressure of compression molding. Similar orientation degree among the composites with different BN contents is also observed.

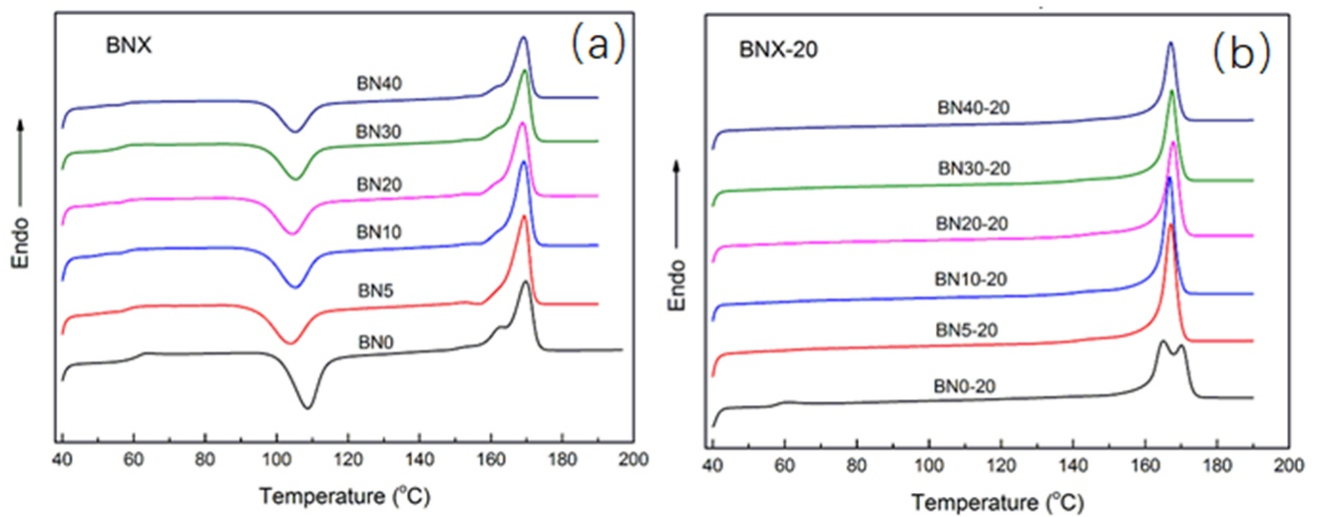


Fig. 1 First melting curves of PLA and PLA/BN composites without (a) and with (b) isothermal treatment at 120 °C.

Table 1 Crystallinity of PLA and PLA/BN blends with and without isothermal crystallization at 120 °C.

BN contents (%)	Crystallinity (%)					
	0	5	10	20	30	40
BNX	0	1	2	3	4	3
BNX-20	49	52	53	53	53	55

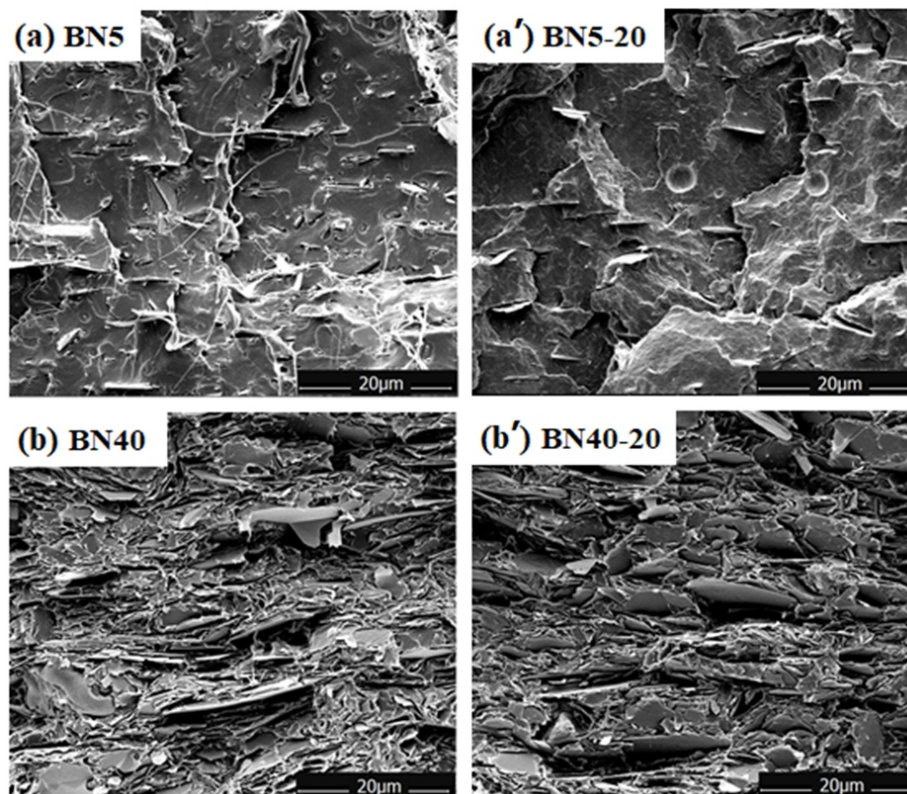


Fig. 2 SEM images of amorphous (a & b) and crystallized (a' & b', 20 min isothermal crystallization at 120 °C) PLA/BN composites with 5 %, and 40 % of BN.

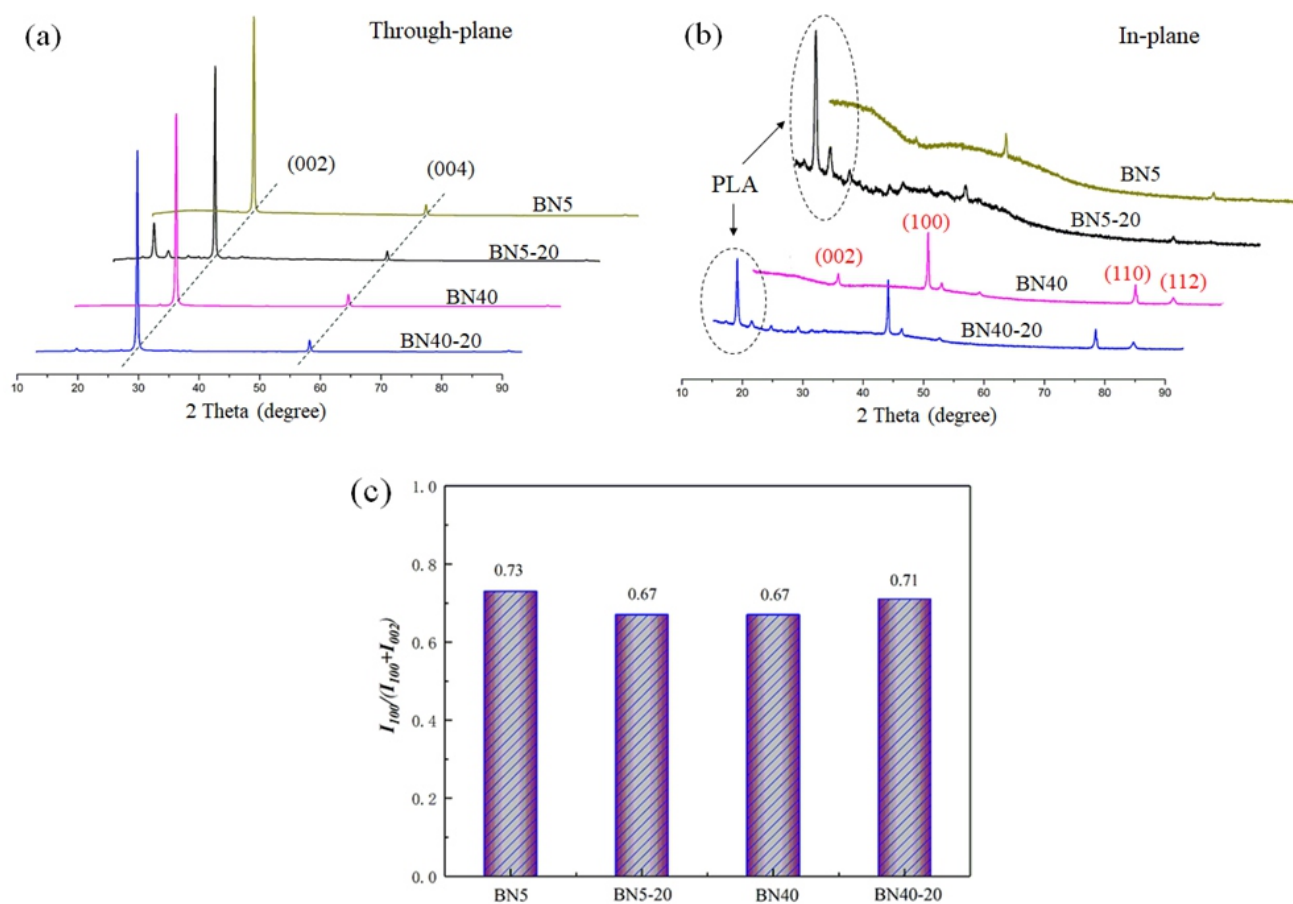


Fig. 3 XRD patterns of PLA/BN composites in the directions of through-plane (a) and (b) in-plane, and (c) orientation factor ($I_{100}/(I_{100} + I_{002})$) of PLA/BN composites.

To further characterize the degree of orientation of BN in PLA/BN composites, the XRD patterns of compressed samples in the in-plane and through-plane directions are shown in Fig. 3 for the composites with 5 % and 40 % BN flakes. The results show that the peaks corresponding to crystalline planes of BN obtained from the through-plane direction (Fig. 3a) and the in-plane direction (Fig. 3b) are completely different, clearly demonstrating that BN flakes are oriented in the polymer matrix.⁹ The $I_{100}/(I_{100} + I_{002})$ ratio extracted from Fig. 3b can be used to characterize the degree of orientation of BN flakes in the PLA matrix and is shown in Fig. 3c. It is observed that isothermal crystallization does not influence the degree of orientation of the BN flakes in the PLA matrix, and the degree of orientation is basically unchanged with the increase in the BN content, with values of approximately 0.7 obtained in all cases. It is noted that when the BN flakes are ideally oriented, the orientation ratio $I_{100}/(I_{100} + I_{002})$ should be 1.0. This means that BN flakes have a high degree of orientation in the PLA matrix by compression molding. The XRD results are well consistent with the SEM observations (Fig. 2). Thus, the degree of orientation will not affect the TC of the samples. It is also observed from Fig. 3(b) that the diffraction peaks of PLA crystals are present in the BN5-20 and BN40-20 samples, but the corresponding peaks are not observed in BN5 and BN40, indicating that the isothermal treatment at 120 °C for 20 min made PLA highly crystallized, while the samples without the isothermal treatment were amorphous. This is also consistent with the DSC test results described above.

TC of the composites can be derived using Eq. (2):

$$k = \alpha \times \rho \times C_p \quad (2)$$

where ρ is the bulk density and C_p is the specific heat at a given pressure. The thermal diffusivity (α) values were measured by the laser flash method which is a noncontact transient thermal measurement method widely used for measuring the thermal diffusivity. The detailed results are listed in Table S1. Using all of these parameters, TC was calculated and shown in Fig. 4. It shows that TCs of crystallized PLA/BN composites in both in-plane and through-plane directions are higher than those of amorphous PLA/BN composites. With crystallization, the phonon mean free path was increased, resulting in the increase of thermal conductivity. Whether the composites were isothermally treated or not, they exhibit increased TC in both in-plane and through-plane directions with increasing BN content. At the same BN content, the TC of PLA/BN composite in the in-plane direction is much higher than that in the through-plane direction. When the content of BN is 40 %, the in-plane TC of crystallized PLA/BN composite reaches 4.7 W/mK, and the through-plane thermal conductivity can even reach 0.8 W/mK. The TC of the BN flake itself in the in-plane direction is greater than its TC in the through-plane direction⁵¹. According to the obtained SEM and XRD results, BN flakes are highly aligned along the in-plane direction of the compression molded specimen, giving rise to the outstanding heat dissipation capability of the composite in the

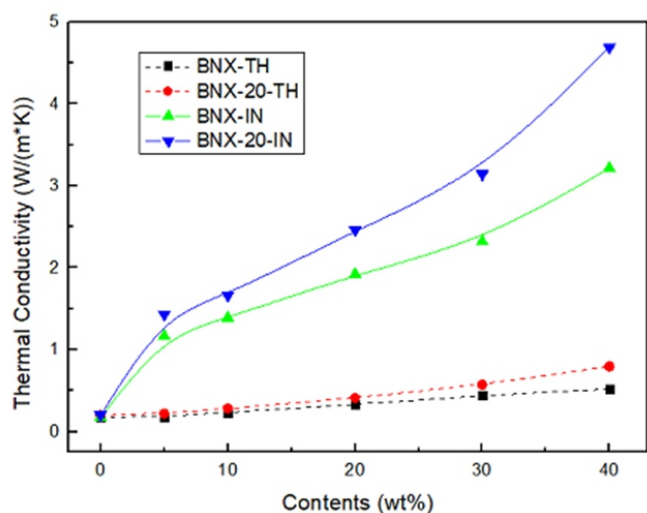


Fig. 4 Thermal conductivity of PLA/BN composites with and without isothermal crystallization at 120 °C for 20 min.

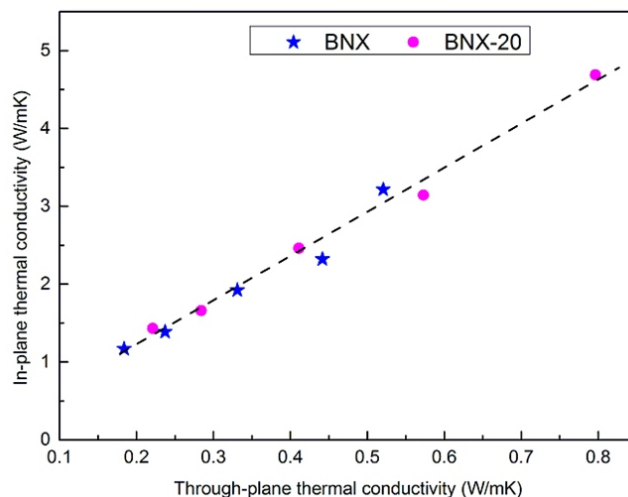


Fig. 5 Relationship between the in-plane and through-plane TCs of PLA/BN composites.

orientation direction.

The TCs of the composite in the different directions show a critical dependence on the orientation of the fillers.⁵² The in-plane TCs of all of the PLA/BN composites are plotted vs. the through-plane TCs in Fig. 5. It is observed that the in-plane TC increases linearly with the through-plane TC, and all of the experimental points fall on a straight line. This demonstrates that the degree of orientation of BN in both BNX and BNX-20 are the same, consistent with the XRD results described above.

To further explore the effect of crystallization on the TC of the composites, the rates of increase in the TCs of the composites were calculated and are presented in Fig. 6. Fig. 6(a) shows the contribution of crystallization to the TC of the composite in both the in-plane and through-plane directions with the increase in the BN content. According to the results, the contributions of crystallization to the TC of the composites are not identical. With increasing BN content, the crystallization contribution to the composite TC becomes more pronounced. The TC of pure PLA was increased by 17 % after crystallization, while the TC of the crystallized PLA/BN composites with 5 % and 40 % content of BN increased by 23 % and 47 %, respectively, in the in-plane direction, and increased by 21 % and 54 %, respectively, in the through-plane direction relative to those of BN5 and BN40.

Fig. 6(b) analyzes the contribution of the BN content to the TCs of crystalline or amorphous PLA/BN composites. The rate of increase in the composite TC increases with increasing BN content for both directions. On the other hand, the increase in the TC values of the crystallized BNX-20 composites with increasing BN content is larger than that of the amorphous BNX composites. When the mass fraction of BN is 5 %, the TC of amorphous PLA/BN is 608 % higher than that of amorphous PLA in the in-plane direction, while the TC of crystallized PLA/BN is 626 % higher than that of crystallized PLA in the in-plane direction, which is 1.03 times that of the amorphous composite. When the content of BN increases to 40 %, the in-plane TC of amorphous PLA/BN is increased by 1848 % compared with that of amorphous PLA, while the in-plane TC of crystallized PLA/BN is increased by 2280 % compared with that of crystallized PLA, which was 1.23 times that of the amorphous composite. This means that PLA crystallization is more effective in promoting the increase in the TC of the composites,

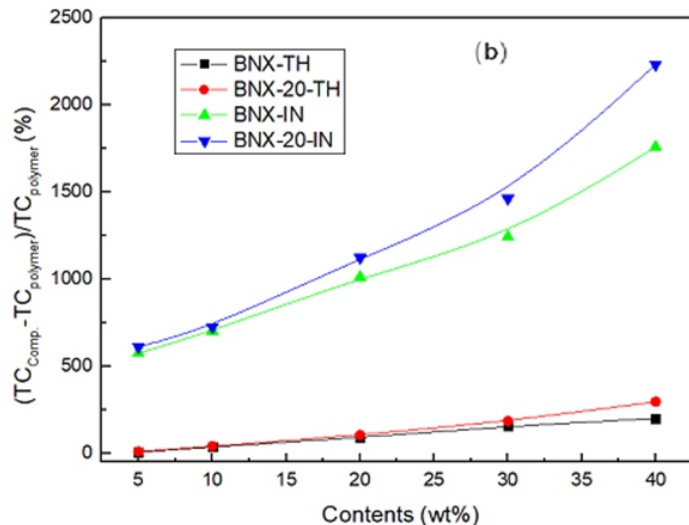
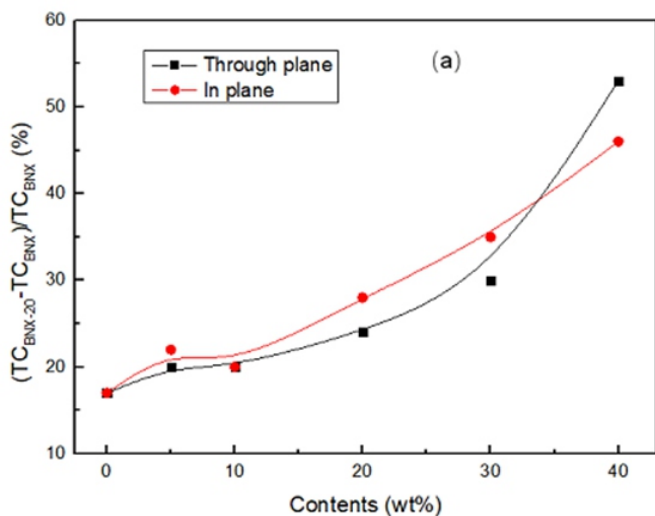


Fig. 6 Enhancement of thermal diffusivity of PLA/BN blends (a) with isothermal crystallization at 120 °C and (b) with the addition of BN.

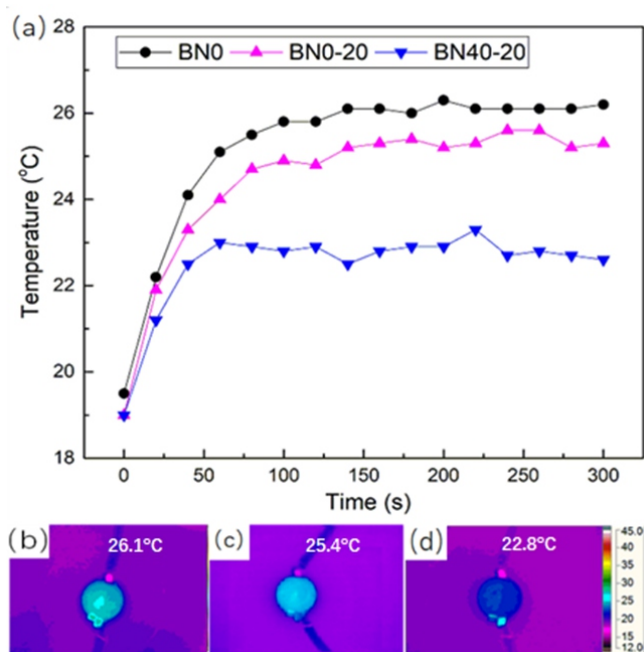


Fig. 7 (a) Temperature variation of LED with working time and the infrared image of working LED by using (b) amorphous PLA (BN0), (c) crystallized PLA (BN0-20) and (d) crystallized PLA/BN (BN40-20) as heat dissipation substrates after 200 s.

and this effectiveness is more obvious at higher filler content.

To visually verify the enhanced TC of crystallized PLA/BN composites, BN0, BN0-20 and BN40-20 specimens were used as the heat dissipation substrates of LED lamps, and the temperature changes of the LED lamps were recorded with an infrared thermal imager. The results are shown in Fig. 7. Fig. 7a shows the temperature variation of a light-emitting-diode (LED) during 300 s. It is clearly observed that the temperature differences of the LED after 50 s is different for different heat dissipation substrates. Because 80-90 % input energy of the LED will be converted to heat and due to the different heat dissipation abilities of the substrates, the temperature of the LED with the amorphous PLA (BN0) as heat dissipation substrate increases sharply, while the temperature shows a much slower increase when the crystallized composite BN40-20 is used as the heat dissipation substrate. After a certain period of time, the temperature of the LED tends to become stable. The time of stabilization is in the order of BN0>BN0-20>BN40-20. Fig. 7 b-d gives the temperature of LEDs after 200s. The LED temperature is stable, and the LED temperature with BN40-20 as the heat dissipation substrate is the lowest, 22.8 °C, while the stable temperatures are 26.1 °C and 25.4 °C when using BN0 and BN0-20 as the heat dissipation substrates. These results also indicate that the crystallization of PLA leads to good TC of PLA/BN composites.

Breakdown strength is a key parameter for the use of an insulation material in practical applications. Fig. 8 shows that crystallization increases the BD strength of pure PLA,³³ but with the addition of BN flakes, the BD strengths of crystallized PLA/BN composites are slightly lower than those of the amorphous PLA/BN composites. Unfortunately, compared with the amorphous PLA/BN composites, the crystallized PLA/BN composites have some small pores in the matrices as observed in Fig. S3, dominating the decrease in the BD strength of the crystallized PLA/BN composites. With increasing content of the BN flakes, the BD strength of the composite first increased and then

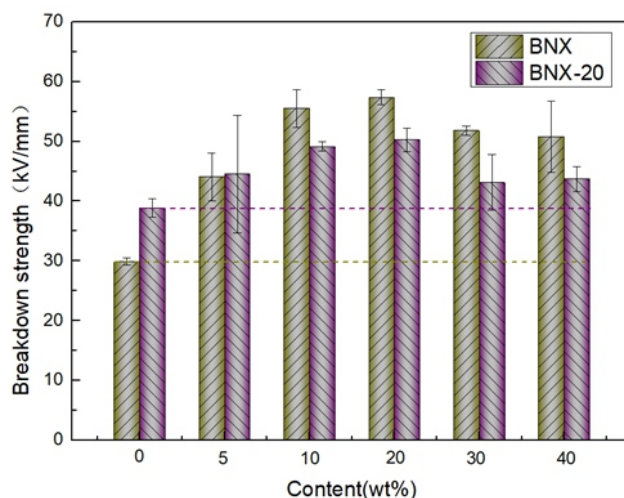


Fig. 8 AC Breakdown strength of PLA/BN composites without and with isothermal crystallization at 120 °C.

decreased slightly, which had nothing to do with PLA crystallization. BN flakes are small platelets, and it is known from the results of SEM and XRD given above that most of the BN flakes are oriented perpendicular to the direction of electric field, effectively preventing the electron transfer through the composites and endowing it with excellent insulating properties. However, taking BN10 & BN10-20 samples as an example, clear gaps between the polymer matrix PLA and BN flakes can be observed in the magnified SEM images (Fig. S3), indicating that the interfacial adhesion of PLA and BN flakes is rather poor. The poor interfacial adhesion decreases the BD strength of the composite. When the BN content is too high, many defects will appear in the composite, resulting in the gradual decrease in the BD strength of the composite. It also shows that the breakdown (BD) strengths of all of the PLA/BN composites were larger than that of PLA. All of the BD strengths of PLA/BN composites are higher than 40 kV/mm, and the highest value reaches as high as 60 kV/mm, showing the excellent insulating properties.

4. Conclusion

PLA/BN composites with different BN contents were melt compounded with a twin-screw extruder. The amorphous and crystallized states of the PLA matrix were tuned by compression molding and isothermal treatment at 120 °C. Morphology of the PLA/BN composites, crystallinity of the PLA matrix, filler orientation, thermal conductivity and breakdown strength of the as-prepared composites were comprehensively examined. The results show that the two series of PLA/BN composites are amorphous and highly crystalline with a crystallinity of approximately 50 %. BN flakes are highly oriented in the PLA matrix along the in-plane direction, and the degree of orientation is independent of the BN contents and PLA crystallization. TC values of the PLA/BN composites increases with increasing BN content and PLA crystallization further improves the TC of the PLA/BN composites, and the improved effectiveness was related to the BN content. A more obvious improvement of both in-plane and through-plane TC is obtained after isothermal crystallization with increasing BN content. The TC of pure PLA is increased by 17 % via crystallization, while the TC of crystallized PLA/BN composite with 5 % and 40 % BN content are increased by 23 % and 47 %, respectively, in the in-plane direction and increased by 21 % and 54 %, respectively, in the through-plane

direction compared to those of BN5 and BN40. Both amorphous and crystalline PLA/BN composites show quite high breakdown strengths. The results provide supporting for the fabrication of highly thermally conductive polymer composites.

Conflict of interest

There are no conflicts to declare.

Acknowledgements

This work was funded by the National Natural Science Foundation of China (51873126, 51721091 and 51422305).

References

1. H. Chen, V.V. Ginzburg, J. Yang, Y. Yang, W. Liu, Y. Huang, L. Du and B. Chen, *Prog. Polym. Sci.*, 2016, **59**, 41-85.
2. Y. Guo, G. Xu, X. Yang, K. Ruan, T. Ma, Q. Zhang, J. Gu, Y. Wu, H. Liu and Z. Guo, *J. Mater. Chem. C*, 2018, **6**, 3004-3015.
3. Z. Han and A. Fina, *Prog. Polym. Sci.*, 2011, **36**, 914-944.
4. C. Huang, X. Qian and R. Yang, 2018, *Mat. Sci. Eng. R.*, 2018, **132**, 1-22.
5. J. Gu, Y. Guo, X. Yang, C. Liang, W. Geng, L. Tang, N. Li and Q. Zhang, *Comp Part A-Appl S.*, 2017, **95**, 267-273.
6. C.P. Feng, L. Chen, F. Wei, H.Y. Ni, J. Chen and W. Yang, *Rsc. Adv.*, 2016, **6**, 65709-65713.
7. Y. L. Yang, X. J. Shi, Y. Z. Feng, S. Li, X. P. Zhou and X. L. Xie, *Comp. Part A-Appl. S.*, 2018, **107**, 657-64.
8. Y. J. Xiao, W. Y. Wang, T. Lin, X. J. Chen, Y. T. Zhang, J. H. Yang, Y. Wang and Z. W. Zhou, *J. Phys. Chem. C*, 2016, **120**, 6344-6355.
9. C. P. Feng, L. Bai, Y. Shao, R. Y. Bao, Z. Y. Liu, M. B. Yang, J. Chen, H. Y. Ni and W. Yang, *Adv. Mater. Interfaces*, 2018, **5**, 1700946.
10. J. Yang, G. Q. Qi, R. Y. Bao, K. Yi, M. Li, L. Peng, Z. Cai, M. B. Yang, D. Wei and W. Yang, *Energy Storage Mater.*, 2018, **13**, 88-95.
11. W. B. Zhang, Z. X. Zhang, J. H. Yang, T. Huang, N. Zhang, X. T. Zheng, Y. Wang and Z. W. Zhou, *Carbon*, 2015, **90**, 242-254.
12. Y. H. Zhao, Y. F. Zhang and S. L. Bai, *Comp. Part A-Appl. S.*, 2016, **85**, 148-55.
13. W. Zhao, J. Kong, H. Liu, Q. Zhuang, J. Gu and Z. Guo, *Nanoscale*, 2016, **8**, 19984-19993.
14. C. P. Feng, L. Bai, R. Y. Bao, Z. Y. Liu, M. B. Yang, J. Chen and W. Yang, *Adv. Compos. Hybrid Mater.*, 2018, **1**, 160-167.
15. J. Xia, G. Zhang, L. Deng, H. Yang, R. Sun and C. P. Wong, *RSC Adv.*, 2015, **5**, 19315-19320.
16. V. Martelli, N. Toccafondi, G. Ventura and *Physica B: Condensed Matter*, 2010, **405**, 4247-4249.
17. T. Zhao, C. Zhang, Z. Du, H. Li and W. Zou, *RSC Adv.*, 2015, **5**, 91516-91523.
18. N. Sun N, J. J. Sun, X. L. Zeng, P. Chen, J. S. Qian and R. Xia, *Comp. Part A-Appl. S.*, 2018, **110**, 45-52.
19. H. Shen, J. Guo, H. Wang, N. Zhao and J. Xu, *ACS Appl. Mater. Inter.*, 2015, **7**, 5701-5708.
20. J. Yang, L. S. Tang, R. Y. Bao, L. Bai, Z.Y. Liu, B. H. Xie, M. B. Yang and W. Yang, *Sol. Energ. Mat. Sol. C.*, 2018, **174**, 56-64.
21. K. Wattanakul, H. Manuspiya and N. Yanumet, *Compos. Mater.*, 2011, **45**, 1967-1980.
22. T. Kusunose, T. Yagi, S.H. Firoz and T. Sekino, *J. Mater. Chem. A*, 2013, **1**, 3440-3445.
23. T. L. Li and S. L. C. Hsu, *J. Phys. Chem. B*, 2010, **114**, 6825-6829.
24. S. M. Yuen, C. C. M. Ma, C. L. Chiang, J. A. Chang, S. W. Huang and S. C. Chen, *Comp. Part A-Appl. S.*, 2007, **38**, 2527-2535.
25. D. Hansen and G. A. Bernier, *Polym. Eng. Sci.*, 1972, **12**, 204-208.
26. C. L. Choy and D. Greig, *J. Phys. C-Solid State Phys.*, 1975, **8**, 3121-3130.
27. C. L. Choy, K.W. Kwok, W. P. Leung, F. P. Lau and J. Polym. Sci. Polym. Phys., 1994, **32**, 1389-1397.
28. J. Yu, B. Sundqvist, B. Tonpheng and O. Andersson, *Polymer*, 2014, **55**, 195-200.
29. C. L. Choy, W. H. Luk and F. C. Chen, *Polymer*, 1978, **19**, 155-162.
30. X. Wang, V. Ho, R. A. Segalman and D. G. Cahill, *Macromolecules*, 2013, **46**, 4937-4943.
31. S. Shen, A. Henry, J. Tong, R. Zheng and G. Chen, *Nat. Nanotechnol.*, 2010, **5**, 251-255.
32. L. Langer, D. Billaud and J. P. Issi, *Solid State Commun.*, 2003, **126**, 353-357.
33. I. Krupa, I. Novák and I. Chodák, *Synthetic Met.*, 2004, **145**, 245-252.
34. T. Zhao and X. Zhang, *Polym. Comp.*, 2017, **38**, 2806-2813.
35. X.T. Meng, V. Bocharova, H. Tekinalp, S.W. Cheng, A. Kisliuk, A.P. Sokolov, V. Kunc and W. H. Peter, S. Ozcan, *Mater. Design.*, 2018, **139**, 188-197.
36. W. Zheng, N. Yan, Y. Zhu, W. Zhao, C. Zhang, H. Zhang, C. Bai, Y. Hu and X. Zhang, *Polym. Chem.*, 2015, **6**, 6088-6095.
37. S. Oza, H. Ning, I. Ferguson and N. Lu, *Comp. B: Eng.*, 2014, **67**, 227-232.
38. N. Lu and S. Oza, *Comp. B: Eng.*, 2013, **44**, 484-490.
39. N. Lu and S. Oza, *Comp. B: Eng.*, 2013, **45**, 1651-1656.
40. H. Gu, H. Zhang, C. Gao, G. Liang, J. Wu and J. Guo, *ES Mater. Manuf.*, 2018, **1**, 3-12.
41. Q. Hao and N. Lu, *ES Mater. Manuf.*, 2018, **1**, 1-2.
42. R. Y. Bao, W. Yang, W. R. Jiang, Z. Y. Liu, B. H. Xie and M. B. Yang, *J. Phys. Chem. B*, 2013, **117**, 3667-3674.
43. L. Bai, X. Zhao, R.Y. Bao, Z.Y. Liu, M. B. Yang and W. Yang, *J. Mater. Sci.*, 2018, **53**, 1-11.
44. H. Takagi, S. Kako, K. Kusano and A. Ousaka, *Adv. Comp. Mater.*, 2007, **16**, 377-384.
45. A. Nakamura and M. Iji, *J. Mater. Sci.*, 2011, **46**, 747-751.
46. M.A.A. Tarawneh, D. Shahdan and S.H. Ahmad, *J. Nanomater.*, 2013, 206961(5pp).
47. J. Huang, Y. Zhu, L. Xu, J. Chen, W. Jiang and X. Nie, *Compos. Sci. Technol.*, 2016, **129**, 160-165.
48. S.G. Mosanenzadeh, S. Khalid, Y. Cui and H.E. Naguib, *Polym. Comp.*, 2016, **37**, 2196-2205.
49. S. M. Lebedev, O. S. Gefle, E. T. Amitov, D. Y. Berchuk and D.V. Zhuravlev, *Polym. Test.*, 2017, **58**, 241-248.
50. A. Guinault, C. Sollogoub, S. Domenek, A. Grandmontagne and V. Ducruet, *Int. J. Mater. Form.*, 2010, **3**, 603-606.
51. Z.P. Xia and Z.Q. Li, *J. Alloy. Comp.*, 2007, **436**, 170-173.
52. K. Uetani, S. Ata, S. Tomonoh, T. Yamada, M. Yumura and K. Hata, *Adv. Mater.*, 2015, **26**, 5857-5862.
53. K. M. Seven, J. M. Cogen, T. Person, J. R. Reffner and J. F. Gilchrist, *J. Appl. Polym. Sci.*, 2018, **135**, 46325 (12pp).